ELECTROSTATIC ANGULAR MICROACTUATOR

Anca TOMESCU, Sorin ANTONIU, Gabriela CIUPRINA
Electrical Engineering Dept., POLITEHNICA University – Bucharest
Petru Gabriel TAFLAN
ROMAVIA – Bucharest

The active electrostatic torque acting on a novel double–action electrostatic angular microactuator is computed by analytical methods of different degrees of approximation and by a finite element numerical method.

INTRODUCTION

Microelectromechanic devices represent a subject of increasing interest due to the increasing number of applications they find in industry, communications, medicine, military, and many other fields made them. In particular, electrostatic angular microactuators [1,2] can be used in the accurate driving of the read/write arm of computer disk devices. The analysis and design of such microactuators has to take into account specific restrictions derived from the manufacturing process specific to the integrated circuit technology.

A preliminary performance evaluation of a microdevice is needed, with a view to establish the range of the proper design and manufacturing requirements. In this respect, the evaluation of the actuation (positioning) characteristic of the angular actuator is essential. The present paper proposes a double–action electrostatic angular microactuator and gives successive approximations of its differential–operation active torque.

DEVICE MODEL AND SIMPLIFYING ASSUMPTIONS

The usual electrostatic angular microactuator [1] is an interdigitated structure consisting in two interleaved conducting radial comb structures, attached to coaxial circumferences, with long comb teeth inserted in each other's comb gaps (fig. 1). The stator teeth are placed at a driving potential V with respect to the null potential V_0 of the rotor teeth. The ensuing attraction between the stator and rotor teeth results in an electric revolving torque, as long as the rotor teeth start from an asymmetrical position with respect to the stator teeth. The rotor reaches an equilibrium position when the electric active torque is balanced by a restoring elastic torque.

The electrostatic microactuator under study [3] is a novel, modified version of the above structure, consisting in two electrically insulated interleaved stator radial comb structures between which the rotor radial comb structure is placed. A unique positioning characteristic is obtained if the rotor teeth are placed in active gaps of the stator teeth separated by idle stator gaps. While the rotor comb structure is placed at null potential $V_0 = 0$, the stator comb structures can be placed at different driving voltages V_1 and V_2, which gives increased control on the positioning characteristic of the actuator (fig. 2).

Some simplifying hypotheses are supposed to apply: 11

1°. The teeth length is much larger than their width and height and than the distances to neighbouring teeth;

2°. The teeth height is fairly larger that the distances to neighbouring teeth;

3°. The idle gaps are sufficiently large so that the electrical potential distribution between them is not influenced by the position of the null potential rotor teeth over their range of rotation;

4°. The electrostatic levitation associated with the presence of the screening conducting plane at null potential under the comb structure is negligible.

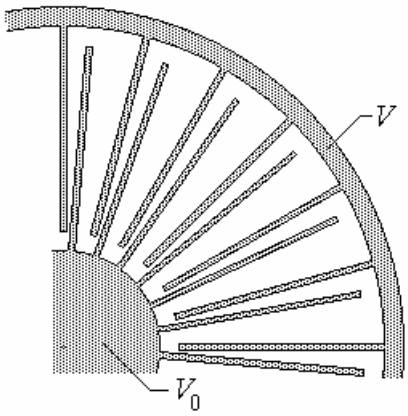

Fig. 1. One–sided mocroactuator

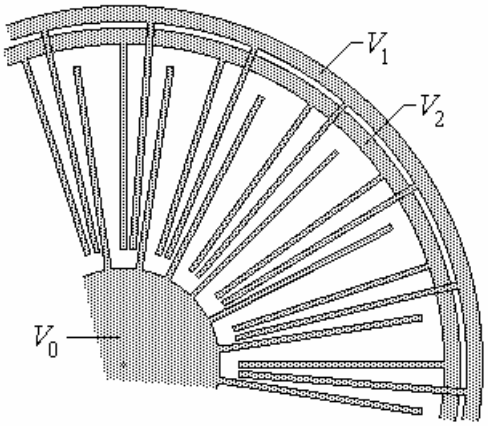

Fig. 2. Two–sided microactuator

The radial placement of the comb teeth imply that it is a three-dimensional problem of the electrostatic field that has to be studied, according with the above simplifying assumptions, for a single active gap of the actuator. However, two approaches to much more manageable two-dimensional treatments of the electric field problem can be considered. First, under the same simplifying hypotheses, the field structure can be considered as that of radially placed plane plates. Second, the radial variation of the field structure can be approximated by a set of plane–parallel field structures at successive radii, followed by an approximate Gauss integration [4] of the resulting torque values. This second approach is also considered for a finite element numerical model.

ANALYTICAL COMPUTATION OF THE ELECTRIC TORQUE

In the first analytical approach, simple approximations of the electric torque are based on the circular arc approximation of the field lines between fixed and mobile zero width teeth [5], for the repetitive actuator structure of the mobile tooth between two energized stator teeth (fig. 3). Taking into account the screening role of the mobile tooth of negligible width, the capacitances to the adjacent fixed teeth are computed separately as

$$C_1 = \frac{\varepsilon_0 HL}{R(\Theta - \theta)} \quad , \quad C_2 = \frac{\varepsilon_0 HL}{R(\Theta + \theta)} \quad , \quad R = \frac{b-a}{\ln(b/a)} = \frac{L}{\ln(b/a)} \quad ,$$

where H is the tooth height, L is the tooth length, Θ is the half angle between stator teeth, θ is the angular displacement of the mobile tooth withg respect to its median position (here, towards the V_1 stator tooth), and R is the mean radius in terms of the limit radii a and b of the mobile tooth. Operating in terms of the electric co–energy W^*, the associated torques result then simply as

$$T = \left.\frac{\partial W^*}{\partial \theta}\right|_{V=\text{ct.}} = \frac{V^2}{2}\frac{\partial C}{\partial \theta} \quad \Rightarrow \quad T_1 = \frac{\varepsilon_0 HLV_1^2}{2R(\Theta - \theta)^2} \quad , \quad T_2 = -\frac{\varepsilon_0 HLV_2^2}{2R(\Theta + \theta)^2} \quad .$$

The dependence of the total electric torque on the revolving angle can be linearized if

a differential control is supposed, corresponding to fixed teeth potentials composed of a common–mode component V and a differential–mode component v ($v < V$), such that

$$V_1 = V + v \quad , \quad V_2 = V - v \quad .$$

The total electric torque per mobile tooth (fig. 4) can thus be written as

$$T = T_1 + T_2 = \frac{2\varepsilon_0 HLV^2}{R\Theta^2}\left(\frac{\theta}{\Theta}+\frac{v}{V}\right)\left(1+\frac{\theta}{\Theta}\frac{v}{V}\right)\left[1-\left(\frac{\theta}{\Theta}\right)^2\right]^{-2} \quad ,$$

and admits successive approximations as

$$T_\theta \cong \frac{2\varepsilon_0 HLV^2}{R\Theta^2}\left\{\frac{v}{V}+\left[1+\left(\frac{v}{V}\right)^2\right]\frac{\theta}{\Theta}\right\} \quad \text{for} \quad \frac{\theta}{\Theta} << 1 \quad ,$$

$$T_v \cong \frac{2\varepsilon_0 HLV^2}{R\Theta^2}\left\{\frac{\theta}{\Theta}+\left[1+\left(\frac{\theta}{\Theta}\right)^2\right]\frac{v}{V}\right\}\left[1-\left(\frac{\theta}{\Theta}\right)^2\right]^{-2} \quad \text{for} \quad \frac{v}{V} << 1 \quad ,$$

$$T_0 \cong \frac{2\varepsilon_0 HLV^2}{R\Theta^2}\left(\frac{\theta}{\Theta}+\frac{v}{V}\right) \quad \text{for} \quad \frac{\theta}{\Theta} << 1 \quad \text{and} \quad \frac{v}{V} << 1 \quad ,$$

the last one only being considered in [1].

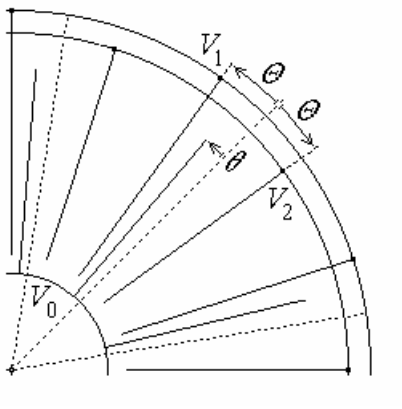

Fig. 3. Radial plates approximation

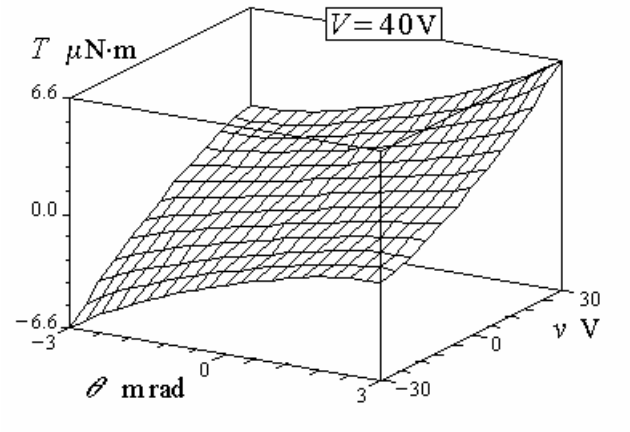

Fig. 4. Electrostatic torque $T(\theta)$

The more detailed second analytical treatment approaches the actuator cell under study as a complete electrostatic system of conductors. An $Oxyz$ reference system is considered, with the *Oyz* plane as the plane of symmetry of the active stator gap and the *Oxy* plane as the basis plane of the fixed teeth, as in fig. 5. The following notations are introduced: tooth height H, mobile/fixed tooth width $G = 2g$, ($G << H$), teeth elevation h, ($h < H$), above the reference plane, distance D, $D \cong (1...2)G$, between mobile–fixed teeth symmetry planes at rest (when no driving potential applied). The interteeth distance obviously depends on the local radius r, so that $D = r\Theta$, where the interteeth angle (at rest) Θ is around $3 \cdot 10^{-3}$ rad. The fixed teeth are at potentials V_1 and V_2, respectively, while the mobile tooth and the screening conducting plane are at null potential.

The complete electrostatic system of conductors is described, in terms of charges and influence coefficients per unit length, by [6,7,8]

$$\begin{cases} q_1 = \alpha_{11} V_1 + \alpha_{12} V_2 \\ q_1 = \alpha_{11} V_1 + \alpha_{12} V_2 \end{cases} ,$$

where

$$\alpha_{11} = \left.\frac{q_1}{V_1}\right|_{V_2=0} , \quad \alpha_{12} = \left.\frac{q_1}{V_2}\right|_{V_1=0} = \left.\frac{q_2}{V_1}\right|_{V_2=0} = \alpha_{21} , \quad \alpha_{22} = \left.\frac{q_2}{V_2}\right|_{V_1=0}$$

and, as a consequence of symmetry, $\alpha_{22}(x) = \alpha_{11}(2D - x)$.

The analytical computation of the influence coefficients is done, in the limits of the field line approximation, in terms of the intermediate variables

$$x_1 = D - G - \theta r , \quad x_2 = D - G + \theta r ,$$

where the deviation of the mobile tooth from its rest position (at potentials $V_1 = V_2 = 0$) is $x = \theta r$.

The influence coefficients per unit length result as

$$\alpha_{12} = \alpha_{21} = -\frac{\varepsilon_0}{2\pi}\left(\frac{4}{3}\ln\frac{\frac{5\pi}{2}G + 2D + \frac{\pi-2}{\pi+2}x_2}{\pi G + 2D + \frac{\pi-2}{\pi+2}x_2} - \ln\frac{\frac{2\pi}{5}H + \frac{\pi}{10}G + \frac{2}{5}D - \frac{1}{5}x_2}{\frac{5\pi}{2}G + 2D + \frac{\pi-2}{\pi+2}x_2} \right) ,$$

$$\alpha_{11} = -\alpha_{12} + \varepsilon_0 \left[\frac{H}{x_1} + \frac{G}{h} - \frac{1}{\pi} + \frac{x_1}{\pi h} + \frac{1}{\pi}\ln\frac{h}{x_1} + \frac{1}{\pi}\ln\frac{x_1 + \pi G}{x_1} + \right.$$

$$\left. + \frac{1}{2\pi}\ln\left(1 + \frac{4\pi\, x_2}{(\pi+2)(\pi G + x_1)} \right) + \frac{2}{\pi}\ln\left\{ 1 + \frac{\pi}{2h}\left[\frac{4H}{5} + \frac{G}{5} - \frac{2}{5\pi}(h - 2D + x_2) \right] \right\} \right] ,$$

$$\alpha_{22}(x_1, x_2) = \alpha_{11}(x_2, x_1) .$$

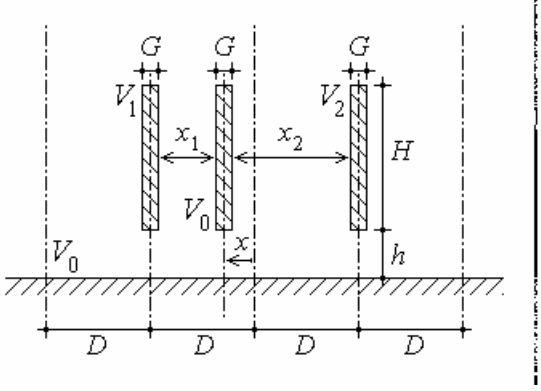

Fig. 5. Plane–parallel approximation

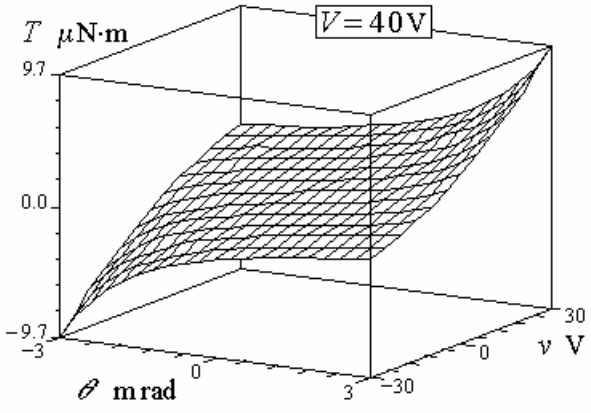

Fig. 6. Electrostatic torque $T(\theta)$

Taking into account the differential control, the local electrostatic torque per unit length on the mobile tooth at a given radius r is then computed as [7,8]

$$T = \frac{(V+v)^2}{2}\frac{\partial \alpha_{11}}{\partial \theta} + \frac{(V+v)^2}{2}\frac{\partial \alpha_{22}}{\partial \theta} + \left(V_1^2 - V_2^2\right)\frac{\partial \alpha_{12}}{\partial \theta} \quad , \quad \frac{\partial}{\partial \theta} = r\left(\frac{\partial}{\partial x_2} - \frac{\partial}{\partial x_1} \right) ,$$

where

$$\frac{\partial \alpha_{12}}{\partial \theta} = -\frac{2\varepsilon_0}{3\pi} \frac{\dfrac{\pi-2}{\pi+2}\dfrac{3\pi G}{2}}{\left(\dfrac{7\pi G}{4}+2D+\dfrac{\pi-2}{\pi+2}x_2\right)^2-\left(\dfrac{3\pi G}{4}\right)^2} -$$

$$-\frac{\varepsilon_0}{2\pi}\left(\frac{1}{2\pi H+\dfrac{\pi G}{2}+2D-x_2}+\frac{\dfrac{\pi-2}{\pi+2}}{\dfrac{5\pi G}{2}+2D+\dfrac{\pi-2}{\pi+2}x_2}\right)+ \quad ,$$

$$\frac{\partial \alpha_{11}}{\partial \theta} = \frac{\partial \alpha_{12}}{\partial \theta} + \varepsilon_0 \frac{2}{(\pi+2)(\pi G+x_1)+4\pi x_2} - \frac{\varepsilon_0}{\pi}\frac{2}{4h+2\pi H+\dfrac{\pi}{2}G+2D-x_2} -$$

$$+\frac{\varepsilon_0}{2\pi}\left(\frac{1}{\pi G+x_1+4\pi x_2/(\pi+2)}-\frac{4}{x_1}+\frac{1}{\pi G+x_1}+\frac{2}{h}-\frac{2\pi H}{x_1^2}\right) \quad ,$$

$$\frac{\partial \alpha_{22}(x_1,x_2)}{\partial \theta} = \frac{\partial \alpha_{11}(x_2,x_1)}{\partial \theta} \quad .$$

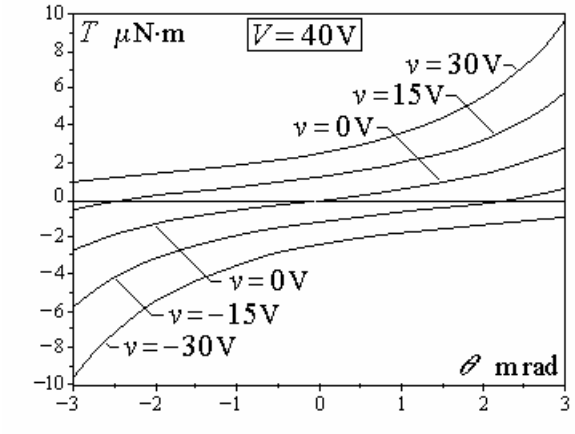

Fig. 7. Electrostatic torque $T(\theta)$

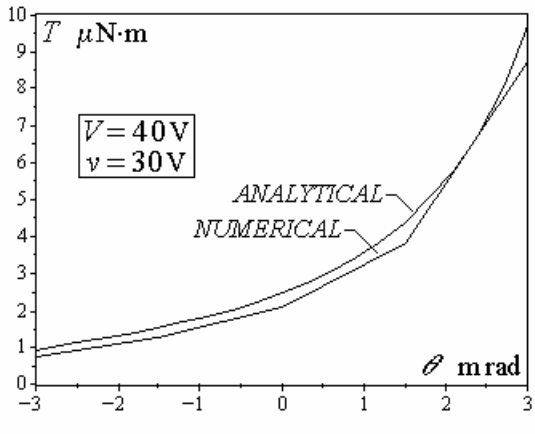

Fig. 8. Electrostatic torque $T(\theta)$

The total torque is computed for the same set of numerical data as before [1] V = 40 V, $v \in [-30,30]$ V, H = 30 μm, h = 10 μm, G = 3 μm, a = 600 μm, b = 1400 μm, Θ = 3 mrad, N = 120 teeth, by using a three–point Gauss approximate integration formula [4],

$$T(\theta) \cong \frac{b-a}{2}\sum_{i=1}^{3} w_i\, T(r_i,\theta) \quad ,$$

and is presented in figs. 6 and 7.

NUMERICAL COMPUTATION OF THE ELECTRIC TORQUE

The finite element numerical model [4] is similar to that used in the second analytical approach (fig. 5): according with the simplifying hypotheses, it is extended laterally by distances D and above the teeth structure by a distance $3(h+H)$. Homogeneous Neumann conditions are enforced on the upper boundaries and given potentials $V = 0$ and $V = V \pm v$ are considered on appropriate conductors along with homogeneous Dirichlet conditions $V = 0$

on the lateral boundaries. For each of the angular positions $\theta = 0$, $\pm\Theta/2$, $\pm\Theta/2$, three values of the radius, $(a+b)/2$ and $(a+b)/2 \pm (b-a)/\sqrt{3}$, were considered.

The finite element solution of the plane–parallel problem gives directly the value of the force per unit length acting locally on the mobile tooth, whence the computation of the electric torque is straightforward, by using the same approximate Gauss integration as before. The total torque is computed for the same set of numerical data as above, and is presented in fig. 8. along with the result of the analytical plane–parallel approximation, for a typical case.

CONCLUSIONS

A novel configuration was proposed for an electrostatic angular microactuator, for which the active electric torque was calculated by two analytical methods and by a finite element numerical method. The analytical methods approached the system as a two–dimensional electric field problem consisting in either a set of radial plates or a set of plane–paralel conductors where the radial variation of distances was accounted for by an approximate Gauss integration. The finite element numerical method was applied for the second model, with a similar post–processing step.

The computed results agree with each other and, in the simplest approximation given by the first analytical approach, is similar to published results [1].

ACKNOWLEDGEMENTS

Thanks are due to the staff of the Numerical Methods Laboratory, and to colleagues in the Group of Theoretical Electrical Engineering of the Electrical Engineering Department, "Politehnica" University of Bucharest.

REFERENCES

1. D.A. Horsley, M.B. Cohn, A. Singh, R. Horowitz, A.P. Pisano, *Design and Fabrication of an Angular Microactuator for Magnetic Disk Drives*, IEEE JMEMS, Vol.7, No.2, June 1998, pp. 141–148.
2. W.A. Johnson, L.K. Warne, *Electrophysics of Micromechanical Comb Actuators*, IEEE JMEMS, Vol 4, No. 1, March 1995, pp. 49–59.
3. P.G. Taflan, *Microactuator electrostatic unghiular*, Graduation thesis, Department of Electrical Engineering, Polytechnic University of Bucharest, 2003.
4. Anca Tomescu, I.B.L. Tomescu, F.M.G. Tomescu, *Modelarea numericã a câmpului electromagnetic*, MatrixRom, Bucharest, 2003.
5. Anca Tomescu, F.M.G. Tomescu, *Analytical Solutions of Electric and Magnetic Fields Using Complex Functions*, 'Politehnica' University of Bucharest, Postgraduate School of Computer Aided Electrical Engineering, Bucharest, 2001.
6. J. Van Bladel, *Electromagnetic Fields*, McGraw-Hill Book Company, New York, 1964.
7. H.A. Haus, J.R. Melcher, *Electromagnetic Fields and Energy*, Prentice Hall, Englewood Cliffs, J.J., 1989.
8. Anca Tomescu, F.M.G. Tomescu, *Bazele electrotehnicii – Sisteme electromagnetice* (*Lecture Notes*), Department of Electronics and Telecommunications, Polytechnic University of Bucharest, 1996.
9. Anca Tomescu, F.M.G. Tomescu, R. Mãrculescu, *Bazele electrotehnicii – Câmp electromagnetic*, MatrixRom, Bucharest, 2002.